



Implementation of a comprehensive ice crystal formation parameterization for cirrus and mixed-phase clouds into the EMAC model (based on MESSy 2.53)

Sara Bacer¹, Sylvia C. Sullivan², Vlassis A. Karydis¹, Donifan Barahona³, Martina Krämer⁴, Athanasios Nenes^{2,5,6,7}, Holger Tost⁸, Alexandra P. Tsimpidi¹, Jos Lelieveld^{1,9}, and Andrea Pozzer¹

¹Atmospheric Chemistry Department, Max Planck Institute for Chemistry, Mainz, Germany

²School of Chemical and Biomolecular Engineering, Georgia Institute of Technology, Atlanta, USA

³NASA Goddard Space Flight Center, Greenbelt, USA

⁴Institut für Energie und Klimaforschung, Forschungszentrum Jülich, Jülich, Germany

⁵School of Earth and Atmospheric Sciences, Georgia Institute of Technology, Atlanta, USA

⁶ICE-HT, Foundation for Research and Technology, Hellas, Greece

⁷IERSD, National Observatory of Athens, Athens, Greece

⁸Institute for Atmospheric Physics, Johannes Gutenberg University Mainz, Mainz, Germany

⁹Energy, Environment and Water Research Center, The Cyprus Institute, Nicosia, Cyprus

Correspondence: Sara Bacer (sara.bacer@mpic.de)

Abstract. A comprehensive ice nucleation parameterization has been implemented in the global chemistry-climate model EMAC to realistically represent ice crystal number concentrations. The parameterization of Barahona and Nenes (2009, hereafter BN09) allows the treatment of ice nucleation, taking into account the competition for water vapour between homogeneous and heterogeneous nucleation and pre-existing ice crystals in cold clouds. Furthermore, the influence of chemically-heterogeneous, polydisperse aerosols is considered via multiple ice nucleating particle spectra, which are included in the parameterization to compute the heterogeneously formed ice crystals. BN09 has been implemented to operate both in the cirrus and in the mixed-phase regimes. Compared to the standard EMAC results, BN09 produces fewer ice crystals in the upper troposphere but higher ice crystal number concentrations in the middle troposphere, especially in the Northern Hemisphere where ice nucleating mineral dust particles are relatively abundant. The comparison with a climatological data set of aircraft measurements shows that BN09 used in the cirrus regime improves the model results and, therefore, is recommended for future EMAC simulations.

1 Introduction

Clouds play an important role in the Earth System by affecting the global radiative energy budget, the hydrologic cycle, the scavenging of gaseous and particulate substances, and by providing a medium for aqueous-phase chemical reactions. Nevertheless, clouds remain one of the most elusive components of the atmospheric system, and their representation in models is one of the major challenges in climate studies (IPCC, 2013; Seinfeld et al., 2016). Compared to the liquid droplet activation process, the ice crystal formation (in mixed-phase and cirrus clouds) is affected by large uncertainties because of the poor



understanding of the chemical and physical principles underlying ice nucleation, the complexity of ice nucleation mechanisms and aerosol-ice interactions (Cantrell and Heymsfield, 2005; Gultepe and Heymsfield, 2016; Heymsfield et al., 2017; Korolev et al., 2017).

Cirrus clouds form at high altitudes and very low temperatures (typically below -35°C) and consist purely of ice crystals. They strongly impact the transport of water vapour entering the stratosphere (Jensen et al., 2013) and play an important role as modulator of radiation fluxes in the global radiative budget: they scatter solar radiation back into the space (albedo effect) and absorb and re-emit longwave terrestrial radiation (greenhouse effect). In addition, mixed-phase clouds consist of both supercooled liquid cloud droplets and ice crystals and generally appear at temperatures above -20°C . Due to the difference between vapour pressure over water and over ice, ice crystals grow at the expense of water droplets (Wegener-Bergeron-Findeisen process), thus, mixed-phase clouds are thermodynamically unstable and can convert into ice-only clouds. Mixed-phase clouds are responsible for the majority of precipitation, lightning and strong storms. The fraction of cloud ice has a profound impact on the cloud forcing in global climate models, one of the reasons why cloud radiative forcing is so diverse and uncertain.

Ice crystal formation takes place via homogeneous and heterogeneous nucleation, depending on environmental conditions (e.g. temperature, supersaturation, vertical velocity) and aerosol populations (i.e. aerosol number concentrations and physico-chemical characteristics) (Pruppacher and Klett, 1997; Kanji et al., 2017; Heymsfield et al., 2017; Korolev et al., 2017). Homogeneous nucleation occurs through the freezing of supercooled liquid droplets at low temperatures ($T < 238\text{ K}$) and high supersaturation over ice (140% – 160%) (Koop et al., 2000). Heterogeneous nucleation refers to the formation of ice on an aerosol surface, which reduces the energy barrier for ice nucleation and lets ice crystals form at lower supersaturations and/or at warmer (subfreezing) temperatures than homogeneous nucleation. The aerosols that lead to the generation of ice crystals are called ice nucleating particles (INPs) and are mostly insoluble, like mineral dust, soot, organics, and biological particles (Pruppacher and Klett, 1997). Heterogeneous nucleation occurs via different mechanisms called “nucleation modes” (deposition, condensation, immersion and contact nucleation). Based on modeling studies, homogeneous nucleation has been considered the dominant process for cirrus formation (e.g. Haag et al., 2003; Gettelman et al., 2012) because the concentration of liquid droplets is higher than that of INPs in the upper troposphere. However, due to the overestimation of vertical velocity this is under debate (Cziczo et al., 2013; Barahona and Nenes, 2011; Barahona et al., 2017). Overall, two different regimes for ice crystal formation are distinguished: the *mixed-phase regime* at subfreezing temperatures between 238 K and 273 K, where ice crystals form exclusively by heterogeneous nucleation and alter the phase composition of the mixed-phase clouds, and the *cirrus regime* at colder temperatures ($T < 238\text{ K}$), where ice crystals originate via heterogeneous and/or homogeneous nucleation to form cirrus clouds.

As heterogeneous nucleation takes place at lower supersaturation than homogeneous nucleation, the available water vapour and degree of supersaturation decrease, reducing or inhibiting the formation of ice crystals from homogeneous nucleation. This competition between homogeneous and heterogeneous nucleation for water vapour drastically affects the ice crystal number concentration (ICNC), even at low INP concentrations (Kärcher and Lohmann, 2003; Spichtinger and Cziczo, 2010). Water vapour can also be reduced by condensation onto pre-existing cloud droplets, depositional growth onto pre-existing ice crystals



and ice crystals carried into the cloud via convective detrainment and advective transport, thus, inhibiting ice nucleation. The impact of pre-existing ice crystals (PREICE) on cirrus clouds can be important when ice crystals have small size and low sedimentation rates at low temperatures (Barahona and Nenes, 2011), leading to optically thinner cirrus clouds characterized by fewer ice crystals with a diverse age distribution and high supersaturation levels, especially in the case of tropical upper troposphere/lowermost stratosphere (UTLS) cirrus (Barahona and Nenes, 2011; Hendricks et al., 2011; Kuebbeler et al., 2014).

Cloud schemes in atmospheric and climate models have evolved from using only macrophysical properties like cloud cover to representing the microphysics explicitly, e.g. formation, evolution, and removal of cloud droplets and ice crystals (Kärcher et al., 2006; Lohmann et al., 2008; Gettelman et al., 2010; Barahona et al., 2014). Including sophisticated schemes in general circulation models (GCMs) allows for a more realistic description of the variability of cloud properties and cloud radiative effects, improving the model climate predictions. Recently, sophisticated parameterizations have been developed, taking into account the aerosol influence on ice formation and different modes of heterogeneous nucleation. Liu and Penner (2005) presented an ice nucleation scheme based on parcel numerical model simulations which considers the competition between homogeneous and heterogeneous nucleation following the classic nucleation theory. Kärcher et al. (2006) developed a physically based parameterization scheme of ice initiation and ice crystal initial growth in cirrus clouds, considering the PREICE effect and allowing for the competition between heterogeneous and homogeneous nucleation. Barahona and Nenes (2009) introduced an ice cloud formation parameterization based on the analytical solution of the cloud parcel model equations, which accounts for the competition between homogeneous and heterogeneous nucleation and the variability of aerosol concentration and composition through a variety of INP spectra. Since then, these parameterizations have been included in GCMs in order to better predict cloud phase partitioning. Hendricks et al. (2011) and Kuebbeler et al. (2014) have implemented the parameterization by Kärcher et al. (2006) into the ECHAM4 and ECHAM5-HAM models, respectively. Liu et al. (2007) and Liu et al. (2012) have implemented the parameterization by Liu and Penner (2005) into the CAM3 and CAM5 models, respectively. Also, Liu et al. (2012) and Barahona et al. (2014) have implemented the scheme of by Barahona and Nenes (2009) in CAM5 and GEOS-5, respectively.

In this study the parameterization of Barahona and Nenes (2009, hereafter BN09) has been implemented into the ECHAM/MESSy Atmospheric Chemistry (EMAC) global model to improve the representation of ice nucleation. The parameterization calculates the competition for water vapour between homogeneous and heterogeneous nucleation and takes into account the variability (in size and chemical composition) of different aerosol species. Moreover, the PREICE effect has been added in the parameterization. BN09 has been used to compute the new ice crystals formed both in the cirrus regime and/or in the mixed-phase regime, and its performance has been compared with the results generated via the standard model configuration. The model evaluation is carried out, paying particular attention to the ice-related results. The paper is organized as follows: the description of the operational model and the BN09 scheme are in Section 2, as well as the information about the implementation work and the simulations run for this study, Section 3 describes the modeled ice-related products, Section 4 contains the evaluation of the model, and Section 5 presents our conclusions.



2 Model description and set-up of simulations

2.1 EMAC model

The EMAC model is a numerical chemistry-climate model (CCM) which describes tropospheric and middle-atmosphere processes and their interactions with ocean, land, and human influences. Such interactions are simulated via dedicated submodels in the MESSy framework (Modular Earth Submodel System, Jöckel et al., 2010), while the 5th generation European Centre Hamburg GCM (ECHAM5, Roeckner et al., 2006) is used as core of the atmospheric dynamics. For the present study we have used ECHAM5 version 5.3.02 and MESSy version 2.53.

The EMAC model has been extensively described and evaluated against in-situ observations and satellite data, e.g. aerosol optical depth, acid deposition, meteorological parameters (e.g. Pozzer et al., 2012, 2015; Karydis et al., 2016; Tsimpidi et al., 2016; Klingmüller et al., 2017). It computes gas-phase species on-line through the MECCA (Module Efficiently Calculating the Chemistry of the Atmosphere) submodel (Sander et al., 2011) and provides a comprehensive treatment of chemical processes and dynamical feedbacks through radiation (Dietmüller et al., 2016). Aerosol microphysics and gas/aerosol partitioning are calculated by the GMXe (Global Modal-aerosol eXtension) submodel (Pringle et al., 2010), a two-moment aerosol module which predicts the number concentration and the mass mixing ratio of the aerosol modes, along with the mixing state. The aerosol size distribution is described by 7 lognormal modes (defined by total number concentration, number mean radius and geometric standard deviation): 4 hydrophilic modes which cover the aerosol size spectrum of nucleation, Aitken, accumulation, and coarse modes, and 3 hydrophobic modes, which have the same size range except for the nucleation mode which is not required. The aerosol composition within each mode is uniform with size (internally mixed) but it varies among modes (externally mixed). The aging of aerosols, through coagulation or condensation of water vapour and sulfuric acid is described by GMXe by transferring aerosols from the externally mixed to the internally mixed modes. Convective and large-scale clouds are separately treated and individually calculated by the submodels CONVECT and CLOUD, respectively. The CLOUD submodel uses a double-moment stratiform cloud microphysics scheme for cloud droplets and ice crystals (Lohmann et al., 1999; Lohmann and Kärcher, 2002; Lohmann et al., 2007) which defines prognostic equations for specific humidity (q_w), liquid cloud mixing ratio (q_l), ice cloud mixing ratio (q_i), cloud droplet number concentration (N_l), and ice crystal number concentration (N_i). The advantage of using a two-moment scheme is that it allows for the explicit computation of cloud particle size distribution, which interacts with radiation and influences the evolution of cloud properties. The diagnostic cloud cover scheme of Sundqvist et al. (1989) based on the grid mean relative humidity is used; it assumes that a grid box is partly covered by clouds when the relative humidity exceeds a threshold and is totally covered when saturation is reached. Other microphysical processes, like phase transitions, autoconversion, aggregation, accretion, evaporation of rain, melting of snow, sedimentation of cloud ice, are taken into account. In the CLOUD submodel, ice clouds form via homogeneous nucleation in the cirrus regime, via immersion and contact freezing in the mixed-phase regime (more details about ice cloud formation are given in the next subsection). The CLOUD submodel is coupled to GMXe to simulate aerosol-cloud interactions. Physical loss processes, like dry deposition, wet deposition, and sedimentation of aerosol, are explicitly considered by the submodels DRYDEP, SCAV and SEDI (Kerkweg et al., 2006; Tost et al., 2006).

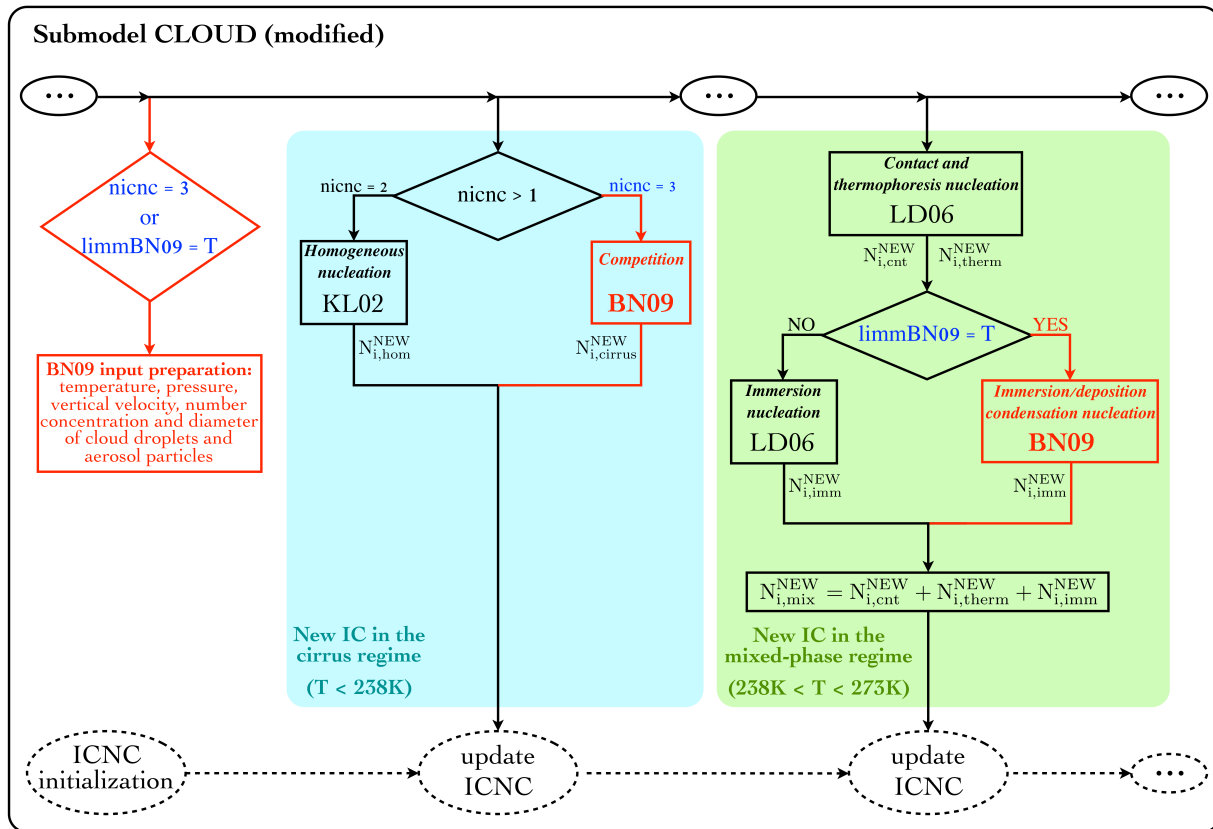


Figure 1. Scheme of the new ice crystal formation in the CLOUD submodel: different ice nucleation schemes can be used in the cirrus and in the mixed-phase regime. $nicnc$ and $limm_BN09$ are variables defined in the namelist-file “cloud.nml”; red parts are new; three dots indicate other processes coded in the CLOUD submodel.

2.2 Default ice nucleation in EMAC

The CLOUD submodel describes the evolution of the prognostic variables which undergo all cloud microphysical processes (e.g. precipitation, deposition, evaporation/sublimation). As far as the formation of the ice crystals is concerned, they are computed via two independent parameterizations, as shown in black in Figure 1.

- 5 In the cirrus regime ($T \leq 238.15$ K) it is assumed that cirrus clouds form exclusively homogeneously using the parameterization by Kärcher and Lohmann (2002, hereafter referred to as KL02). Such parameterization computes the newly formed ice crystals via homogeneous nucleation ($N_{i,hom}^{NEW}$) of supercooled solution droplets and allows supersaturation with respect to ice. Alternatively, it is possible to use the parameterization by Kärcher and Lohmann (2003) to simulate cirrus formation via pure heterogeneous freezing, however, by default the model operates with KL02, under the assumption that the dominant freezing
- 10 mechanism for cirrus clouds is homogeneous nucleation.



In the mixed-phase regime ($238.15 \text{ K} < T \leq 273.15 \text{ K}$) heterogeneous nucleation occurs via immersion ($N_{i,imm}^{NEW}$) and contact ($N_{i,cont}^{NEW}$) freezing as described in Lohmann and Diehl (2006, hereafter referred to as LD06). Insoluble dust can initiate contact nucleation in the presence of supercooled water droplets following the parameterization of Levkov et al. (1992). Soluble dust and black carbon can act as immersion nuclei, according to the stochastic freezing hypothesis described in Diehl and Wurzler (2004). Possibly, contact freezing via thermophoresis can be included ($N_{i,therm}^{NEW}$), but it is usually not considered (i.e. $N_{i,therm}^{NEW} = 0$) since its contribution is negligible (Lohmann and Hoose, 2009). The Wegener-Bergeron-Findeisen (WBF) process at subfreezing temperatures is parameterized, so liquid water is forced to evaporate from cloud droplets and deposit onto existing ice crystals.

In the CLOUD submodel, a single updraft velocity (w) is used for the whole grid cell, although w can vary strongly in reality within the cell horizontal dimension (e.g. Guo et al., 2008). This is a simplification which is commonly used by GCMs, nevertheless, important progress has been recently achieved on this front to describe the subgrid-scale variability of updraft velocity using high resolution simulations (Barahona et al., 2017). In EMAC, the subgrid-scale variability of vertical velocity is introduced by a turbulent component (w_{sub}) which depends on the subgrid-scale turbulent kinetic energy (TKE) described by Brinkop and Roeckner (1995), such that $w_{sub} = 0.7\sqrt{TKE}$. The vertical velocity is given by the sum of the grid mean vertical velocity (\bar{w}) and the turbulent contribution: $w = \bar{w} + 0.7\sqrt{TKE}$ (Kärcher and Lohmann, 2002). Zhou et al. (2016) analysed the effect of different updraft velocity representations on ice number concentrations and showed that using w_{sub} overestimates the ice crystal number concentrations at temperatures below 205 K, but agrees better with the observations at higher temperatures. Given the importance of updraft velocities for ice formation (Donner et al., 2016; Sullivan et al., 2016), future studies could implement a complete probability distribution of updrafts.

Finally, the influence of the pre-existing ice particles is not taken into account. The only precaution adopted by the CLOUD submodel is the reduction of the number of aerosol particles available for ice nucleation by the existing ice particle number.

2.3 Ice nucleation parameterization BN09

In order to improve the representation of ice nucleation in the current EMAC model, we have implemented the ice crystal formation parameterization introduced by Barahona and Nenes (2009). In this Section we briefly describe the parametrization and its implementation into the EMAC model.

2.3.1 Scheme characteristics

The BN09 parameterization is computationally efficient and suitable for large-scale atmospheric models. It explicitly considers the competition for water vapour between homogeneous and heterogeneous nucleation in the cirrus regime, the influence of polydisperse (in size and composition) aerosols acting as INPs, and allows to use different heterogeneous nucleation spectra.

The BN09 algorithm can be divided in three subsequent parts. First, the limiting number of INPs (N_{lim}) needed to inhibit homogeneous nucleation is computed if temperatures are below 238 K. Indeed, at such cold temperatures homogeneous and heterogeneous nucleation compete for water vapour decreasing ice supersaturation. When INPs exceed N_{lim} and the maximum supersaturation (s_{max}) that develops in the cloud parcel is less than the threshold for homogeneous nucleation (s_{hom}),



homogeneous nucleation is suppressed and ice crystals are formed only heterogeneously. N_{lim} is determined by computing the number of INPs required to drop s_{max} below s_{hom} .

In the second step, ice crystals nucleated heterogeneously ($N_{i,hct}$) are computed via the selected INP spectrum at s_{hom} , then two cases can follow. If the condition $N_{i,hct}(s_{hom}) \geq N_{lim}$ is satisfied, ice crystals are formed only heterogeneously at s_{max} (i.e. $N_{i,hct}(s_{max})$), as homogeneous nucleation is suppressed. Here, the s_{max} is determined using a bisection method to balance the supersaturation within the air parcel. If $N_{i,hct}(s_{hom}) < N_{lim}$, the competition between homogeneous and heterogeneous nucleation is simulated. The ice crystals nucleated homogeneously ($N_{i,hom}$) are determined via the homogeneous nucleation parameterization of Barahona and Nenes (2008, 2009) (hereafter BNhom):

$$f_c = f_{c,hom} \left[1 - \left(\frac{N_{i,hct}(s_{hom})}{N_{lim}} \right)^{3/2} \right]^{3/2} \quad (1)$$

$$N_{i,hom} = N_c e^{-f_c} (1 - e^{-f_c}) \quad (2)$$

where N_c is the number concentration of supercooled liquid cloud droplets and f_c is the fraction of freezing soluble aerosol. The first factor of f_c (i.e. $f_{c,hom}$) is defined by Barahona and Nenes (2008), while the second factor is the correction introduced by Barahona and Nenes (2009) to take into account the reduction of the probability of homogeneous nucleation due to the change in the droplet size distribution during crystal formation.

Third, the total concentration of new ice crystals formed in the cirrus regime ($N_{i,cirrus}^{NEW}$) is determined by the contribution of both heterogeneous and homogeneous nucleation, i.e. $N_{i,cirrus}^{NEW} = N_{i,hct} + N_{i,hom}$ (see Figure 1). On the other hand, if the temperature is higher than 238 K, the algorithm uses the INP spectrum to compute $N_{i,hct}(s_{max})$.

It is important to stress that the BN09 code actually includes five INP spectra to deal with heterogeneous nucleation (as mentioned before) and these are described by (i) Meyers et al. (1992), (ii) Phillips et al. (2007), (iii) Phillips et al. (2008), (iv) Phillips et al. (2013), and (v) Barahona and Nenes (2009). They are all empirically based except the latter, which is derived from the classic nucleation theory (CNT). Sensitivity studies have shown that global means of ICNC vary up to a factor twenty according the INP spectrum used (when the competition between homogeneous and heterogeneous nucleation is taken into account) and that empirical based spectra better agree with observations, while the CNT spectrum overestimates the number of ice crystals (Barahona et al., 2010; Sullivan et al., 2016). Therefore, the simulations described in Subsection 2.4 use the spectrum by Phillips et al. (2013, hereafter referred to as P13) to simulate heterogeneous nucleation, since it better agrees with observations (Sullivan et al., 2016). P13 is the improved version of Phillips et al. (2008), a comprehensive empirical formulation which takes into account the surface area contribution of different insoluble aerosols (with diameters larger than 0.1 μm) to deposition and immersion/condensation nucleation modes, besides the temperature and the supersaturation with respect to ice. The aerosol particles responsible for ice nucleation are divided in four groups: mineral dust (DU), inorganic black carbon (BC), biological aerosols (BIO), and soluble organics (OCsol). Dust and soot, the aerosol species considered in



this work, contribute to determine $N_{i,het}$ in the following way:

$$n_{INP,X} = \int_{\log(0.1\mu\text{m})}^{\infty} \left[1 - e^{-\mu_X(D_X, S_i, T)} \right] \frac{dn_X}{d\log D_X} d\log D_X \quad X = DU, BC; \quad T < 273.15 \text{ K} \quad (3)$$

$$N_{i,het}(s_{max}) = \sum_{X=1}^{N_X} n_{INP,X} \quad (4)$$

where $n_{INP,X}$ is the number concentration of INPs activated at a saturation ratio with respect to ice S_i and temperature T for the aerosol species X , μ_X represents the mean number of activated ice embryos per insoluble aerosol particle of species X with diameter $D_X > 0.1 \mu\text{m}$, n_X is the number concentration of aerosol particles of species X , and N_X is the number of different aerosol species. Equation (3) can be further extended for biological aerosols and soluble organics, as shown in Phillips et al. (2013), and $N_{i,het}$ denotes the new ice crystals formed via deposition and immersion/condensation.

Summarizing (see Figure 1), according to BN09 the new ice crystals formed in the cirrus regime are:

$$N_{i,cirrus}^{NEW} = \begin{cases} N_{i,hom} + N_{i,het}(s_{hom}) & N_{i,het}(s_{hom}) < N_{lim}, s_{max} = s_{hom} \\ N_{i,het}(s_{max}) & N_{i,het}(s_{hom}) \geq N_{lim}, s_{max} < s_{hom} \end{cases} \quad (5)$$

while in the mixed-phase regime, as a result of deposition and immersion/condensation nucleation, they are computed as:

$$N_{i,imm}^{NEW} = N_{i,het}(s_{max}) \quad (6)$$

2.3.2 Implementation

The BN09 parameterization has been added in the MESSy framework in order to compute the newly formed ice crystals in the cirrus regime and/or in the mixed-phase regime. The input variables of BN09 are: temperature (T , [K]); pressure (P , [Pa]); width of the vertical velocity distribution (w_{sub} , [m s^{-1}]) with upper limit 3 m s^{-1} and lower limit 0.001 m s^{-1} (like in Sullivan et al., 2016); number concentration of activated cloud droplets (N_c , [m^{-3}]), dry diameter of sulfate in Aitken soluble mode (D_c , [m], see Appendix A) and standard deviation of Aitken soluble mode (σ_c); number concentrations (N_X , [m^{-3}]), geometric mean dry diameters (D_M , [m]), and lognormal standard deviations (σ_M) of X aerosol species (which can be DU, BC, OCsol, BIO, depending on the choice of the INP spectrum). Given the internally mixed representation of aerosols in EMAC, the diameters D_M are not distinguished among aerosol species but only among the M modes (Aitken (K), accumulation (A), coarse (C)) which the species belong to. Similarly, the standard deviations σ_M are differentiated only by mode (in EMAC $\sigma_K = \sigma_A = 1.59$ and $\sigma_C = 2.0$). The output variables of BN09 are number concentration and radius of new ice crystals. They are weighted over a Gaussian updraft velocity distribution, with mean 0.1 cm s^{-1} and standard deviation equal to w_{sub} , in order to account for the sub-grid variability (Sullivan et al., 2016).

A schematic overview of how BN09 has been implemented into the EMAC chemistry-climate model through the CLOUD submodel is shown in Figure 1. Moreover, the PREICE effect has been included in the BN09 code. This effect is parameterized by reducing the vertical velocity for ice nucleation (w_{sub}) by a factor depending on the pre-existing ice crystal number



concentration and size, limiting the expansion cooling. We compute such “corrected” vertical velocity ($w_{sub,pre}$) as defined by equation (24) in Barahona et al. (2014). Further information about the implementation is given in Appendix A. Overall, BN09 is a scheme more realistic than KL02 and LD06 which improves the ice nucleation in EMAC by taking into account processes which were previously neglected (e.g. water vapour competition, influence of polydisperse aerosols, PREICE effect).

5 2.4 Setup of simulations

In this study EMAC simulations have been carried out with T42L31ECMWF resolution, which corresponds to a spherical truncation of T42 (i.e. quadratic Gaussian grid of approx. $2.8^\circ \times 2.8^\circ$ in latitude and longitude) and 31 vertical hybrid pressure levels up to 10 hPa (approx. 25 km) at the lower stratosphere. All simulations have been run for 6 years (1 year as spin-up time plus 5 years for the analyses) using year 2000 emissions (GFEDv3.1 from van der Werf et al., 2010 for biomass burning and CMIP5-RCP4.5 from Clarke et al., 2007 for biomass burning). Prescribed climatologies of sea surface temperatures (SST) and sea-ice concentrations (SIC) from AMIP (30 years: 1980-2009) have been used as boundary conditions, and climatologies of aerosols (CMIP5-RCP4.5, GFEDv3.1, AEROCOM) have been used to take into account the interactions with radiation and heterogeneous chemistry. Daily means have been saved as output.

Table 1 lists all simulations of this study and summarises their main characteristics. The default experiment (DEF or KL+LD) is performed with the standard configuration of the EMAC model, i.e. using the parameterization by Kärcher and Lohmann (2002) for cirrus clouds and the parameterization by Lohmann and Diehl (2006) for immersion nucleation in the mixed-phase regime. The “unified activation framework” (UAF) of Kumar et al. (2011) is used as cloud droplet formation parameterization, like in Karydis et al. (2017). UAF is an advanced physically based parametrization which takes into account the effects of adsorption and absorption of dust on the cloud condensation nuclei (CCN) activity. In order to investigate the model performance using the BN09 scheme, we carried out three other experiments where BN09 operates in the two cloud regimes in different combinations: BN09 computing the new ice crystals in the cirrus regime (BN+LD), in the mixed-phase regime (KL+BN), and in both regimes (BN+BN).

In all experiments, contact nucleation is computed according to LD06, while thermophoresis contact nucleation is not considered since its contribution is negligible (as commented in Subsection 2.2). The P13 spectrum is used to simulate heterogeneous nucleation whenever BN09 is called (for the reasons explained in Subsection 2.3). Biological and organic aerosol contributions (which are potential inputs for P13) are turned off to compare all the tests under the same conditions, since LD06 includes only dust and soot.

3 Model results

3.1 Annual zonal means

The annual zonal means of ICNC and ice water content (IWC) are shown as a function of altitude in Figure 2, where the isolines at 273 K and 238 K indicate the approximate bounds of cirrus and mixed-phase regimes. Despite the different ice



Experiment name	Ice nucleation scheme	
	<i>Cirrus regime</i>	<i>Mixed-phase regime</i>
KL+LD or DEF	KL02, pure homogeneous nucleation	LD06, immersion nucleation
BN+LD	BN09, competition and PREICE	
KL+BN	KL02, pure homogeneous nucleation	BN09, immersion/condensation
BN+BN	BN09, competition and PREICE	and deposition nucleation via P13

Table 1. All experiments carried out in this study.

nucleation parameterizations, ICNCs show similar qualitative patterns in all simulations, indicating the important role of atmospheric dynamics. Their numbers decrease towards lower altitudes because the homogeneous nucleation rate reduces with increasing temperature, while they are much higher over the mid-latitudes in the Northern Hemisphere (NH) because of larger INP concentrations (Figure 2a). Looking at the relative changes, we note that ICNCs computed with BN09 in the cirrus regime are much lower than the default ICNCs in the upper troposphere and at high latitudes in the Southern Hemisphere (SH), where they are lower by up to 80% (Figure 2b). This is likely due to the PREICE effect predicted by BN09, as it has been shown that BNhom and KL02 produce the same order of magnitude of ICNC (Barahona and Nenes, 2008). On the other hand, ICNCs increase at lower altitudes and especially in the NH. This is due to higher TKE at lower altitudes, which impacts the updraft velocity and increases heterogeneous nucleation contribution, particularly in the NH (not shown) with larger sources of efficient ice-nucleating mineral dust. Indeed, it has been demonstrated that heterogeneous nucleation is important in the NH (Cziczo et al., 2009), where cirrus clouds are formed from a combination of homogeneous and heterogeneous processes, while homogeneous nucleation dominates in the upper troposphere in the tropics and in the SH (Haag et al., 2003; Liu et al., 2012; Barahona et al., 2017). Overall, as commented later in Subsection 4.1, the total ICNC globally decreases. The changes produced by applying BN09 in the mixed-phase regime (Figure 2c) result from the different heterogeneous ice nucleation parameterizations used to simulate immersion nucleation, P13 vs. LD06. The changes are especially evident in the NH (more than 40%), where mineral dust is more abundant than in the SH. Overall, the ICNC differences obtained using the various ice schemes in the mixed-phase regime are smaller (mostly within $\pm 20\%$) than in the cirrus regime. Finally, the simulation using BN09 in both regimes combines the effects described so far (Figure 2d). Since cirrus clouds do not occur throughout the year, we present in the supplement file (Figure S1) the ICNC seasonal means for summer (June-July-August, JJA) and winter (December-January-February, DJF). The seasonal analysis helps to understand why there is cirrus occurrence at temperatures warmer than 238 K, showing that the ICNC growth in the mixed-phase region predicted by BN+LD is actually very small, as expected given that the ice scheme used in the mixed-phase regime is the same as the default simulation.

IWC decreases with increasing temperature, where ICNC is lower (Krämer et al., 2016), and we find three areas with higher values over the mid-latitudes in both hemispheres and the tropics (Figure 2e). Overall, the pattern is quite symmetrical between the two hemispheres, except at high latitudes in the NH, where IWC is slightly higher because of the higher values of ICNC. The relative changes in Figure 2f show a pattern very similar to Figure 2b, therefore, when BN09 is used in the cirrus regime



IWC decreases with ICNC. On the other hand, BN09 in the mixed-phase regime produces slightly lower IWC (up to 20%) in areas where ICNC increases, especially in the NH at high latitudes (Figure 2g). On average, P13 calculates a larger INP number, and hence smaller ice crystals, than LD06. The TKE updraft formulation may also predict higher supersaturations that allow a contribution of numerous but smaller crystals from heterogeneous nucleation. Finally, BN+BN in Figure 2h simulates an overall reduction of IWC except in the three areas with higher values of IWC described in Figure 2e.

3.2 Global distributions

Figure 3 shows the global distributions of ICNC annual means at two different altitudes: 200 hPa (cirrus regime) and 600 hPa (mixed-phase regime). ICNCs in the cirrus regime mostly follow the precipitation pattern, while other areas with higher ICNC ($> 500 \text{ L}^{-1}$) correspond to mountainous regions, e.g. the Rocky Mountains, Andes, Tibetan Plateau (Figure 3a). At 200 hPa, the annual global mean of ICNC is about 200 L^{-1} ($\sim 390 \text{ L}^{-1}$ over land and $\sim 124 \text{ L}^{-1}$ over ocean). The relative changes clearly show that BN09 used in the cirrus regime (Figure 3b, d) reduces ICNC (up to 60%) worldwide with respect to the default experiment, except over Indian and Indonesian areas. The ICNC annual global mean decreases to 137 L^{-1} (i.e. more than 30%) in BN+LD. Such a reduction occurs mostly because of the PREICE effect in the SH and the competition in the NH. On the contrary, KL+BN is characterised by a general increase of ICNC (Figure 3c). However, most of the areas with strong positive changes (larger than 60%) correspond to regions characterized by low ICNC ($< 30 \text{ L}^{-1}$), thus, the global annual mean increases just up to 218 L^{-1} (i.e. +9%). At 600 hPa, ICNC increases towards high latitudes, in particular over Greenland (up to 2000 L^{-1}) and Antarctica (mostly $> 2000 \text{ L}^{-1}$) (Figure 3e). The annual global mean is about 53 L^{-1} , which means about one quarter with respect to the ICNC global mean at 200 hPa. Interestingly, the ice nucleation scheme used in the cirrus regime affects the ICNC at the mixed-phase regime altitudes. In fact, as shown in Figure 2b, BN+LD predicts higher ICNCs especially in the NH (Figure 3f). However, the largest differences occur in areas where ICNCs are very low and slightly affect the absolute ICNC values. As a result, the annual global mean actually decreases to 47 L^{-1} because of the negative contribution in the SH. Figure 3g also shows strong positive biases, but ICNCs do not change globally (52 L^{-1}). In general, we find that the ICNC in the mixed-phase regime is less sensitive to the ice nucleation scheme changes than the ICNC in the cirrus regime. Vertically integrated ice crystal number concentrations ($ICNC_{burden}$, Figure S2 in the supplement file) clearly show that concentrations are higher over continents ($\sim 48 \cdot 10^8 \text{ m}^{-2}$), where vertical updrafts are stronger and aerosol concentrations more abundant, than over oceans ($\sim 11 \cdot 10^8 \text{ m}^{-2}$).

IWC at 200 hPa and 600 hPa (Figure 4) presents a pattern qualitatively similar to the ICNCs at the corresponding heights. Nevertheless, two interesting features appear. First, the high IWC values ($> 10 \text{ mg kg}^{-1}$) over the Indonesian region at 200 hPa, where ICNCs are not particularly high. Maritime updraft velocities are weaker, and recent work has shown that there are important oceanic sources of INP (e.g. DeMott et al., 2016). These effects may combine to produce few large crystals in this Southern Pacific region. Second, IWC at 600 hPa is rather low over Antarctica, which is instead one of the regions with the highest ICNC (likely because of the low water vapour concentration). The relative changes of IWC with respect to the default simulation (Figure S3 in the supplement file) approximately follow the changes obtained for ICNC, i.e. IWC reduces where

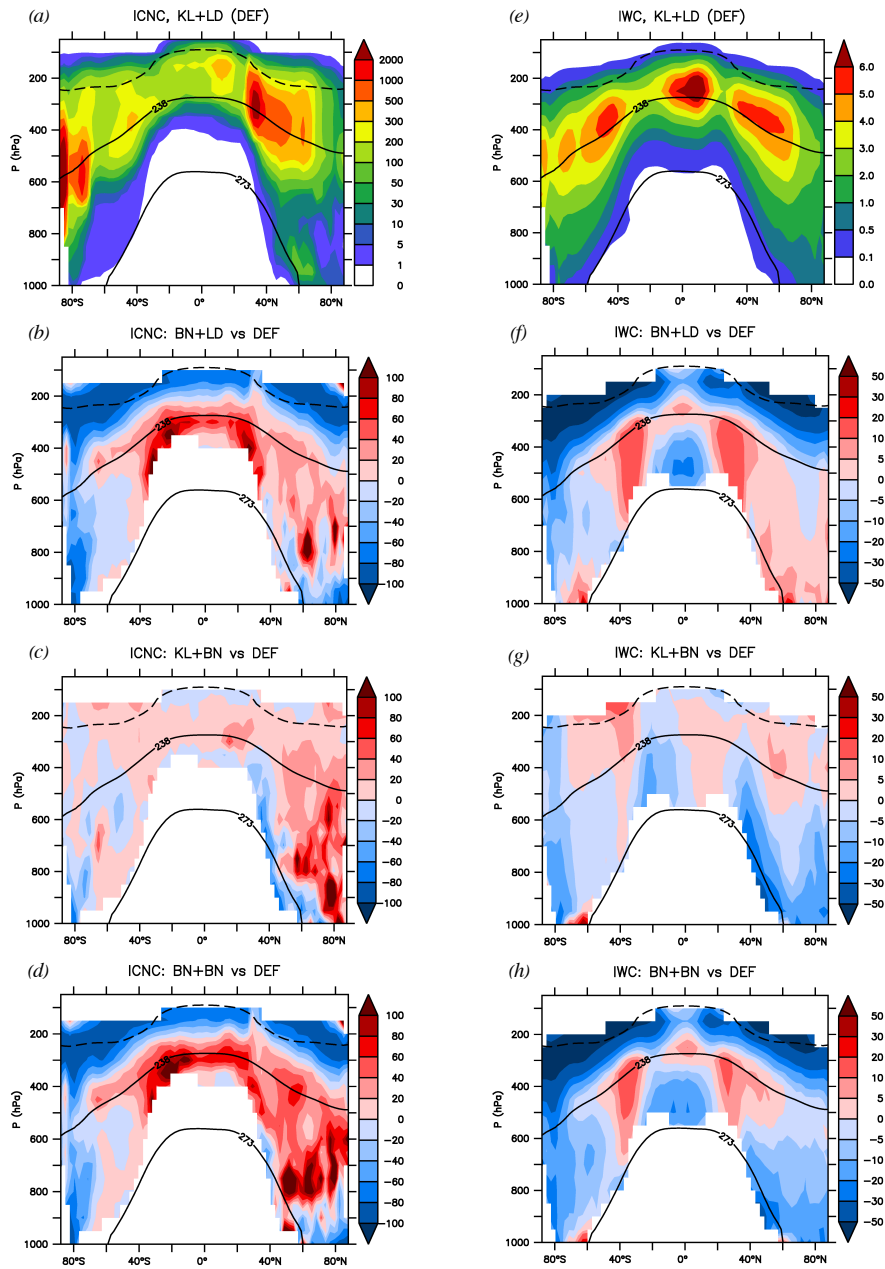


Figure 2. Annual zonal means of ice crystal number concentration ($ICNC$, [L^{-1}]) and non-precipitable ice water content (IWC , [$mg\ kg^{-1}$]) for the default simulation $KL+LD$ and the relative percentage changes of $BN+LD$, $KL+BN$, and $BN+BN$ with respect to it (i.e. $(experiment - DEF)/|DEF| \cdot 100$), computed where $ICNC^{DEF} \geq 1\ L^{-1}$ and $IWC^{DEF} \geq 0.1\ mg\ kg^{-1}$. The isolines at 273 K and 238 K and the tropopause (dotted line) are annual means.



ICNC decreases and vice versa, but using BN09 in the cirrus regime dramatically increases IWC in equatorial regions at 200 hPa.

4 Model comparisons and observations

An evaluation of the double-moment cloud microphysics scheme used by ECHAM5 was presented in Lohmann et al. (2007, 2008) and Lohmann and Hoose (2009), applying the two-moment aerosol microphysics scheme HAM (Stier et al., 2005). Lauer et al. (2007) and Righi et al. (2013, 2015, 2016) showed an evaluation of the CLOUD submodel in conjunction with the aerosol microphysics submodel MADE (Ackermann et al., 1998). Although Tost (2017) evaluated the CLOUD submodel in combination with the GMXe submodel, in this section we extend the comparison with various observations.

4.1 Annual global means

Table 2 shows an overview of the global annual means of cloud microphysical and radiative parameters and fluxes computed for different observations and for all experiments, and the percentage changes of these values with respect to the default simulation. The global vertically integrated ice crystal number concentration changes considerably depending on the ice scheme used in the cirrus regime and in mixed-phase regime. When BN09 operates in the cirrus regime, $ICNC_{burden}$ decreases by 10% due to the competition between homogeneous and heterogeneous nucleation and the PREICE effect (a similar result has been found also by Liu et al., 2012, Kuebbeler et al., 2014, and Shi et al., 2015). On the other hand, $ICNC_{burden}$ increases by almost 7% when BN09 is used in the mixed-phase regime, i.e. when P13 simulates heterogeneous nucleation. On a large scale, these effects offset each other in BN+BN, where the global annual mean is basically unchanged with respect to the default simulation. Overall, all $ICNC_{burden}$ values are very close to the global annual means found by Lohmann et al. (2008) and Kuebbeler et al. (2014), while they are an order of magnitude higher compared to the results of Wang and Penner (2010) and Shi et al. (2015). Unfortunately, there are no global observations of ICNC, but we will provide a statistical comparison with flight measurements in Section 4.2. Vertically integrated cloud droplet number concentration ($CDNC_{burden}$) is not influenced by the choice of the ice nucleation scheme, and the values are comparable with the observations and previous modeling studies (e.g. Lohmann et al., 2007; Hoose et al., 2008; Salzmänn et al., 2010; Wang and Penner, 2010; Kuebbeler et al., 2014; Shi et al., 2015).

The ice water path (IWP) is quite sensitive to the ice scheme used. It decreases by almost 7% when BN09 is used in the cirrus regime, similarly to what has been found in Kuebbeler et al. (2014) and Lohmann et al. (2008), who compared, respectively, simulations assuming pure homogeneous nucleation against simulations including water vapour competition and against simulations considering homogeneous and heterogeneous nucleation (in different grid boxes). Overall, the model underestimates the IWP, also found in other studies that applied ECHAM (e.g. Lohmann et al., 2008; Lohmann and Hoose, 2009; Kuebbeler et al., 2014). The liquid water path (LWP) estimates derived from satellite observations vary substantially, between 23 and 87 g/m². The modeled results fall within this range and the one indicated as acceptable by Mauritsen et al. (2012), which is 50 – 80 g/m². The LWP variations among the experiments are much smaller than the IWP variations.

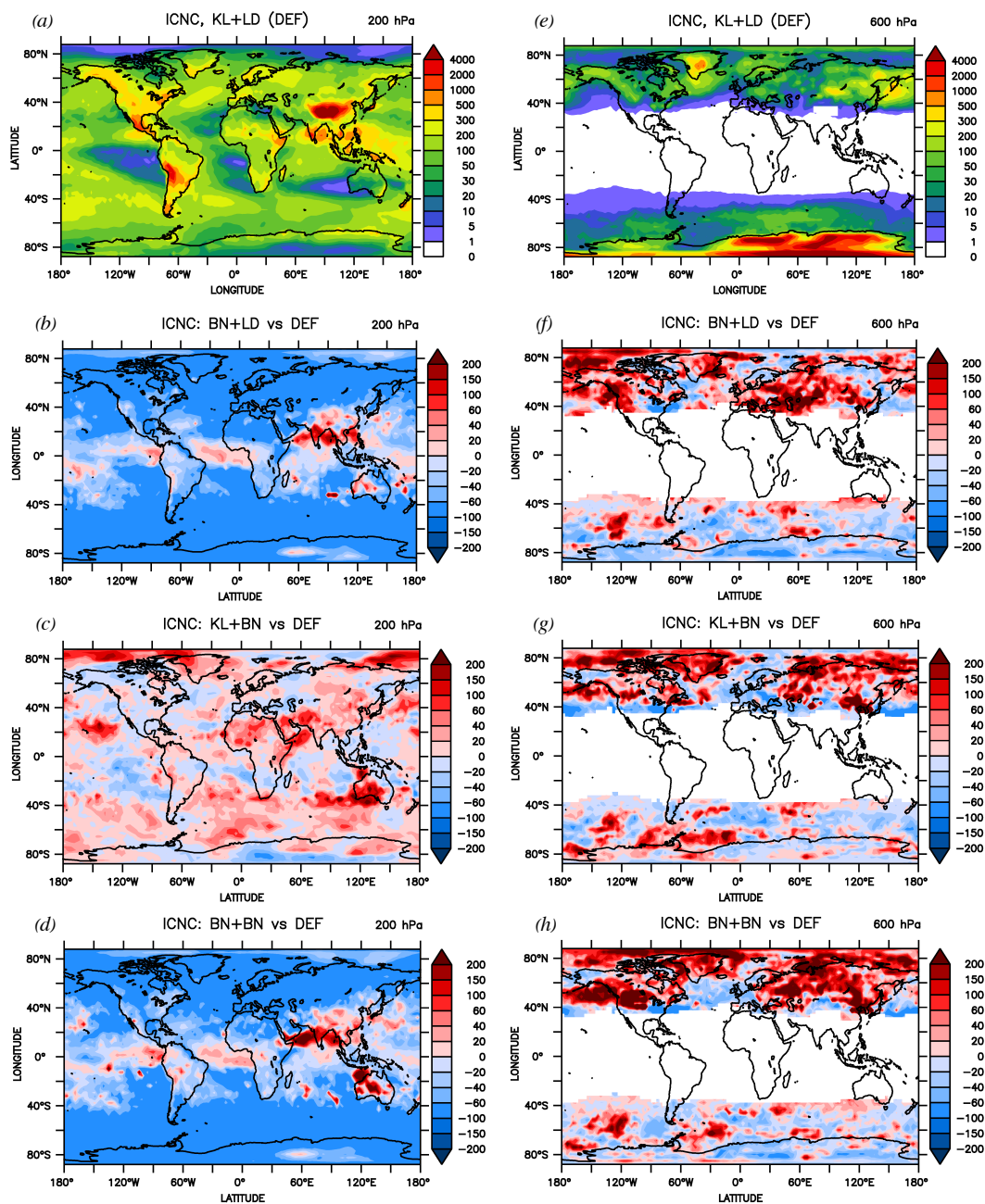


Figure 3. Annual means of ice crystal number concentration ($ICNC$, [L^{-1}]) at 200 hPa (cirrus regime) and 600 hPa (mixed-phase regime) for the default simulation KL+LD and the relative percentage changes of BN+LD, KL+BN, and BN+BN with respect to it (i.e. $(experiment - DEF)/|DEF| \cdot 100$).

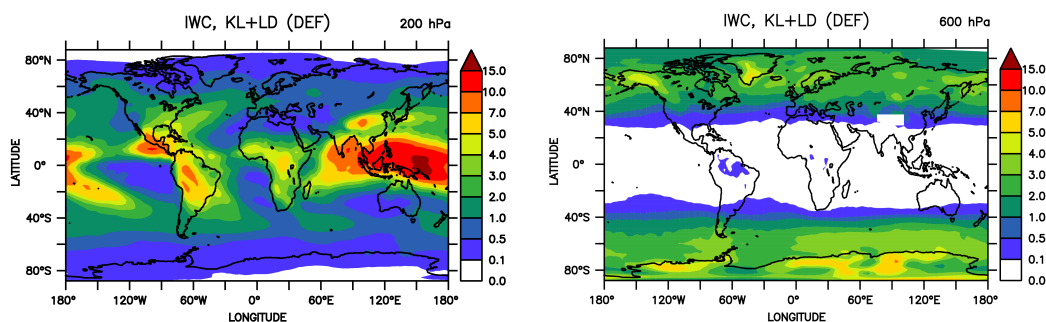


Figure 4. Annual means of ice water content (IWC , [mg kg^{-1}]) at 200 hPa (cirrus regime) and 600 hPa (mixed-phase regime) for the default simulation KL+LD.

The absolute values of the shortwave cloud radiative effect ($SCRE$) and longwave cloud radiative effect ($LCRE$) are higher than those derived from satellite data, especially when KL02 is employed in the cirrus regime. However, when the net cloud radiative effect ($NCRE$) is computed, the same simulations with KL02 in the cirrus regime are closer to the observations. From at the percentage changes it is evident that the cloud radiative effects are sensitive to the ice nucleation scheme used for cirrus clouds. Indeed, $SCRE$ increases more than 5% with BN09 because of the less efficient scattering of shortwave radiation by fewer and larger crystals. More importantly, $LWCR$ decreases more than 14% in BN+LD because cirrus clouds, at the same, can trap less longwave radiation in the Earth-atmpsphere system. As a result, the $NCRE$ diminishes, and the cooling effect is enhanced.

The total cloud cover (TCC) is slightly overestimated by the model (likely explaining why the cloud radiative forcing is high despite IWP being half of the observed values). However, Mauritsen et al. (2012) assert that a global model is acceptable if TCC is higher than 60%. The changes with respect to the default simulation are very low (below 2%), and the biggest change is in BN+LD where TCC reduces by 1.39%, since lower ICNCs leads to higher sedimentation rates. Finally, the model tends to overestimate the total precipitation (P_{tot}), i.e. the sum of large scale and convective precipitations, but this has also been found with other global models (e.g. Barahona et al., 2014 with GEOS-5, Shi et al., 2015 with CAM5, and Lohmann et al., 2008 and Kuebbeler et al., 2014 with ECHAM as well). When BN09 is used in the cirrus regime, P_{tot} grows by 4% especially because of the increase of the convective precipitation contribution (the large scale precipitation of all simulations remain almost constant). BN09 predicts fewer and larger crystals over tropical, continental regions where previous studies show that the majority of precipitation initiates in the ice phase (e.g. Mülmenstädt et al., 2015).

The annual zonal means of vertically integrated number concentration of ice crystals and cloud droplets, ice water path, liquid water path, shortwave and longwave cloud radiative effect, and total cloud cover are shown in Figure S4 (in the supplement file) and are comparable with the literature cited before. The annual zonal mean profiles show clearly that the simulations using the same ice nucleation scheme in the cirrus regime are very close to each other, i.e. KL+LD and KL+BN, and BN+LD and BN+BN (as already visible in Table 2).



	KL+LD (DEF)	BN+LD (2)	KL+BN (3)	BN+BN (4)	OBSERVATIONS	2 vs DEF [%]	3 vs DEF [%]	4 vs DEF [%]
CDNC _{burden} [10^{10} m^{-2}]	4.15	4.21	4.12	4.18	4.01 ^(A)	1.32	-0.72	0.72
ICNC _{burden} [10^8 m^{-2}]	21.86	19.61	23.33	21.75		-10.29	6.72	-0.50
LWP [g/m^2]	75.37	72.73	76.58	74.62	87.1 ^(B) , 23.0 ^(C)	-3.50	1.61	-1.00
IWP [g/m^2]	12.79	11.95	12.70	11.85	25.8 ^(C) , 29.0 ^(D)	-6.57	-0.70	-7.35
SCRE [W/m^2]	-57.81	-54.83	-58.07	-55.37	-48.50 ⁽¹⁾ , -47.14 ⁽²⁾ , -47.04 ⁽³⁾	5.15	-0.45	4.22
LCRE [W/m^2]	33.95	28.90	34.40	29.52	29.42 ⁽¹⁾ , 26.87 ⁽²⁾ , 26.00 ⁽³⁾	-14.87	1.33	-13.05
NCRE [W/m^2]	-23.87	-25.93	-23.67	-25.84	-19.07 ⁽¹⁾ , -19.7 ⁽²⁾ , -21.04 ⁽³⁾	-8.63	0.84	-8.25
TCC [%]	70.01	69.04	70.04	69.23	66.83 ⁽⁴⁾ , 66.7 ⁽⁵⁾	-1.39	0.04	-1.11
P _{tot} [mm/day]	2.902	3.032	2.892	3.024	2.624 ⁽⁶⁾ , 2.669 ⁽⁷⁾	4.48	-0.34	4.20

Table 2. Global annual means for simulations and observations. Shown are vertically integrated cloud droplet number concentration ($CDNC_{burden}$), vertically integrated ice crystal number concentration ($ICNC_{burden}$), liquid water path (LWP), and ice water path (IWP) averaged over the whole spatial grid, shortwave cloud radiative effect ($SCRE$), longwave cloud radiative effect ($LCRE$), net cloud radiative effect ($NCRE$), total cloud cover (TCC), and total precipitation (P_{tot}). The sixth column contains the annual global means computed using the satellite data from ERBE 1985-1990⁽¹⁾ and 2000-2006⁽⁴⁾, CERES-SYN1deg 2004-2010⁽²⁾, CERES-EBAF 2000-2016⁽³⁾, MODIS-TERRA 2004-2008⁽⁵⁾, CMAP 1970-2016⁽⁶⁾, GPCP 1979-2009⁽⁷⁾, and global means taken from the literature: ^(A) is derived from AVHRR data (Gettelman et al., 2010), ^(B) from NOAA-9 and NOAA-10 data (Han et al., 1994), ^(C) from CloudSat data (Li et al., 2012), and ^(D) from ISCCP data (Storelvmo et al., 2008). Last three columns on the right show the percentage changes of the experiments 2, 3, 4 with respect to the default simulation, i.e. $(experiment - DEF)/|DEF| \cdot 100$.

Overall, the model performs well with respect to observations and the literature. Mostly, the experiments do not yield evident differences among each other at the global scale, as regional variations may cancel out, and there are clear effects on SCRE and LCRE from changing the cirrus ice nucleation scheme. As there is not a clear indication which simulation performs better, in the next subsection we extend our analysis including a statistical comparison with aircraft measurements.

5 4.2 Comparison with aircraft measurements

The validation of climate models with measurements from field experiments or aircraft campaigns is always limited by the fact that the models have difficulties to capture individual meteorological events. Nevertheless, here we consider the big collection of aircraft measurements recorded in 15 years, between 1999 and 2014 (*Krämer: personal communication, not yet published*). 18 field campaigns (113 total number of flights and about 127 hours in cirrus clouds) covered Europe, Australia, Africa, Seychelles, Brazil, USA, Costa Rica, and tropical Pacific (i.e. between 25°S and 75°N) in the temperature range of 185 – 243 K. This extensive observational data set is compared to the modeled in-cloud ICNC in Figure 5 (*left*). The observed ICNC varies between 8 and 80 L^{-1} over the entire temperature range, and the lower and upper quartiles vary between 0.6 and 300 L^{-1} .

Again, the simulations can be grouped in two sets according to the ice nucleation scheme used in the cirrus regime, i.e. KL+LD/KL+BN and BN+LD/BN+BN, because of their similarities. At temperatures below 205 K, the first set strongly underestimates (at least three orders of magnitude) the observed ICNC, while the second set shows good agreement with the



measurements. The strong ICNC underestimation at cold temperatures has been already pointed out by Kuebbeler et al. (2014). They used the parameterization of Kärcher et al. (2006) with the ECHAM5-HAM GCM, and indicated a too low vertical velocity as the reason for such underestimation. From Figure 5 (*left*) we deduce that KL02 produces too low ICNCs in cold cirrus clouds (for $T < 205$ K) as well, while BN09 works better at such low temperatures. Between 205 K and 230 K there is a reverse tendency. The simulations KL+LD and KL+BN are closer to the observations and lie within the observed 25th – 75th percentiles at temperatures higher than 215 K. The simulations with BN09 in the cirrus regime underestimate the observations and are outside the 25th – 75th percentiles in the interval 205 – 222 K. In this case, the changes between the simulations indicate that competitive nucleation and PREICE effects are overestimated in warm cirrus clouds (for $T > 205$ K). Finally, all simulations show the same profiles at temperatures higher than 230 K: they overestimates the ICNC by one order of magnitude in the range 230 – 240 K but agree again with the observations at higher temperatures. We reiterate that ICNC is highly dependent on the vertical velocity which is usually poorly represented in terms of spatial and temporal variability (Barahona et al., 2017).

Overall, the simulations BN+LD and BN+BN are always within the observed 5th – 95th percentiles and, for most of the temperature range, within the 25th – 75th percentiles. They show a negative bias (below the 25th percentile) only between 205 K and 220 K but agree particularly well with the measurements at temperatures lower than 200 K. On the contrary, the simulations which consider only homogeneous nucleation in the cirrus regime show a large underestimation (even below the 5th percentile) at temperatures lower than 210 K, however, they are always within the observed 25th – 75th percentiles at higher temperatures. ECHAM5 has strongly underestimated ICNC at low temperatures thus far (Kuebbeler et al., 2014), while most modeling studies (e.g. Wang and Penner, 2010, Liu et al., 2012, and Shi et al., 2015) have shown overestimations. The implementation of BN09 has helped to alleviate this dramatic underestimation of cold cirrus ICNC (in agreement with Barahona et al., 2017).

For further information, in Figure 5 (*right*) we also show the modeled in-cloud ICNC in the mixed-phase regime (i.e. in the temperature range of 238 – 273 K), considering the same latitudes as the case before (25°S - 75°N). The distinctive features are the ICNC decrease with increasing temperatures and a positive “bulge” between 265 K and 270 K caused by secondary ice production (rime splintering). The simulations do not show any significant difference among each other, meaning that the parameterizations P13 and LD06 produce similar ICNC via pure heterogeneous nucleation. The modeled ICNCs are in quite good agreement with two data sets of flight measurements taken from the projects Winter Icing Storms Project (WISP-94) and Ice in Clouds Experiment-Layer Clouds (ICE-L). It is important to stress that this comparison is less accurate than the previous one because the observations here are much more limited both in time and in space than the extensive observational data used for the cirrus regime. Additionally, it should be noted that the measurements actually concern INPs. At mixed-phase conditions, the INP number is usually not so high that supersaturation is depleted before all particles have nucleated, so INP concentrations and ICNCs should generally correspond.

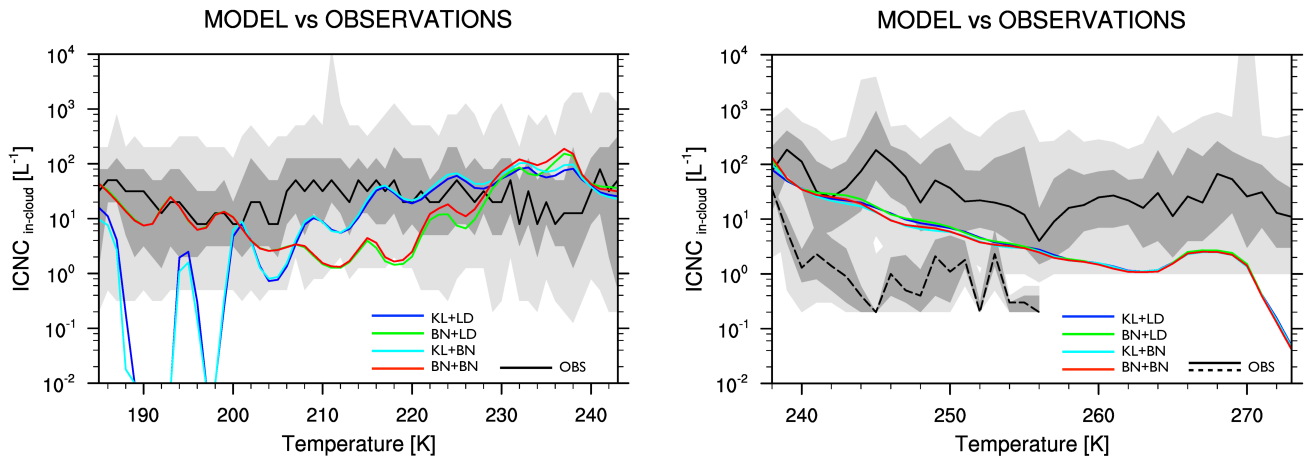


Figure 5. In-cloud ice crystal number concentrations ($ICNC_{in-cloud}$, [L^{-1}]) versus temperature for modeled results and flight measurements. Medians are computed for modeled results (using daily means between 25°S and 75°N) and observations, for each 1 K temperature bin. They are shown with colored lines: KL+LD (blue), BN+LD (green), KL+BN (light blue), and BN+BN (red), observations (black). The dark gray color indicates the observations between 25th and 75th percentiles, while the light gray color indicates the observations between 5th and 95th. (Left) Cirrus regime: the modeled medians are computed approximately in the range of 4–20 km height, the observations come from Krämer (*personal communication, not yet published*). (Right) Mixed-phase regime: the modeled medians are computed approximately in the range of 0–20 km height, the observations belong to the projects WISP-94 (solid line) and ICE-L (dashed line).

5 Conclusions

In this study we have implemented the ice nucleation scheme of Barahona and Nenes (2009) into the chemistry climate model EMAC. The parameterization takes into account the water vapour competition between homogeneous and heterogeneous nucleation and has been modified to consider also the depositional growth of pre-existing ice crystals. Heterogeneous nucleation can be computed through different INP spectra, and we have chosen the empirical INP spectrum of Phillips et al. (2013) for our experiments. We have tested the BN09 scheme operating in the the cirrus and/or in the mixed-phase regimes and compared the results with the standard configuration of the model, which assumes that cirrus clouds form via pure homogeneous nucleation (Kärcher and Lohmann, 2002) and uses the immersion nucleation parameterization of Lohmann and Diehl (2006) for the mixed-phase clouds.

Focusing on the ice-related results, e.g. ICNC and IWC, we found that using BN09 in the cirrus regime strongly reduces the total ICNC worldwide because of the competition and PREICE effects, however, increases ICNC along the tropics. In contrast, BN09 in the mixed-phase regime produces slightly higher ICNCs, especially in the NH where mineral dust particles are more abundant. At the global scale the experiments have not shown evident differences, although the simulations using the same parameterization in the cirrus regime were discernable from the others, particularly in the reduction of longwave cloud forcing.



Overall, all modeled results agree well with global observations and the literature data. The comparison made with flight measurements has demonstrated that ICNCs are more realistically simulated when BN09 is used in the cirrus regime. The experiments BN+LD and BN+BN are always within the observed 5th – 95th percentiles and perform particularly well at low temperatures, in contrast to the default model which severely underestimates ICNC in cold cirrus clouds.

5 Considering that BN09 (1) takes into account processes which were previously neglected, (2) performs generally better, and (3) consumes the same computational resources as the standard version of the model, we conclude that BN09 is the recommended ice nucleation scheme to be applied in future EMAC simulations. Since P13 incorporates the ice-nucleating ability of different aerosol species (dust, soot, bioaerosols and soluble organics) and simulates both deposition and immersion/condensation nucleation, it is also suggested to be used with BN09.

10 *Code and data availability.* The Modular Earth Submodel System (MESSy) is continuously further developed and applied by a consortium of institutions. The usage of MESSy and access to the source code is licensed to all affiliates of institutions, which are members of the MESSy Consortium. Institutions can become a member of the MESSy Consortium by signing the MESSy Memorandum of Understanding. More information can be found on the MESSy Consortium Website (<http://www.messy-interface.org>). All code modifications presented in this article will be included in the next version of MESSy.

15 Appendix A

In this Appendix we provide some additional technical information about the implementation of BN09 into the EMAC model. The BN09 parameterization has been added as a Fortran95 module in the submodel core layer (SMCL) of MESSy (named as `messy_cloud_ice_BN09.f90`). BN09 operates in the cirrus regime and/or in the mixed-phase regime according to the calls made in the CLOUD submodel (`messy_cloud_lohmann10.f90`). As shown in Figure 1, BN09 computes the newly formed
20 ice crystals in the cirrus regime when `nicnc=3` and in the mixed-phase regime when `limm_BN09=.TRUE.`, where `nicnc` and `limm_BN09` are variables defined in the namelist-file `cloud.nml` (the setup of `cloud.nml` for the simulation BN+BN is shown in Table S5 as an example).

Other changes made during the implementation are the following ones.

- 25 – *Temperature threshold.* The original BN09 assumes the value 235 K as temperature threshold between the two regimes, while the CLOUD submodel uses the value 238.15 K. For consistency, we use the second threshold as limit condition to call BN09, and we change the original threshold of BN09 to the value 238.15 K inside the BN09 code.
- 30 – *Number concentration and diameter of cloud droplets.* The original BN09 computes the cloud droplet number concentration starting from the number concentration of sulfate aerosol in the Aitken mode. However, since the EMAC model computes the activated cloud droplet number concentration via other parameterizations (e.g. Abdul-Razzak and Ghan, 2000; Lin and Leaitch, 1997; Karydis et al., 2017), we provide BN09 with such variable (neglecting the corresponding computations inside the BN09 code). Unfortunately, these parameterizations do not compute the diameter of the new



cloud droplets, therefore, BN09 still computes the diameter using the wet diameter of sulfate aerosol in the Aitken mode (i.e. D_c).

Competing interests. The authors declare that they have no conflict of interest.

Acknowledgements. We would like to thank Dr. Mattia Righi from the German Aerospace Center (DLR) for the discussion on the modeled results. We acknowledge the usage of the Max Planck Computing and Data Facility (MPCDF) for the simulations performed in this work. Sylvia C. Sullivan and Athanasios Nenes acknowledge funding from a NASA Earth and Space Science Fellowship (NNX13AN74H), a NASA MAP grant (NNX13AP63G), and a DOE EaSM grant (SC0007145). Moreover, Athanasios Nenes acknowledges funding by the European Research Council Consolidator Grant 726165 (PyroTRACH), Vlassis A. Karydis acknowledges support from an FP7 Marie Curie Career Integration Grant (project reference 618349), Holger Tost acknowledges funding from the Carl-Zeiss foundation, and Alexandra P. Tsimpidi acknowledges support from a DFG individual grand programme (project reference TS 335/2-1). We acknowledge the NCAR - Earth Observing Laboratory for providing the data from the WISP94 (<https://data.eol.ucar.edu/dataset/236.001>) and the ICE-L (<https://data.eol.ucar.edu/dataset/105.021>) projects, under the sponsorship of the National Science Foundation. Finally, we acknowledge the use of the programs Ferret (product of the NOAA's Pacific Marine Environmental Laboratory, <http://ferret.pmel.noaa.gov/Ferret/>) and NCL (product of the Computational and Information Systems Laboratory at the NCAR, <https://www.ncl.ucar.edu/>) for the analyses and graphics in this paper.



References

- Abdul-Razzak, H. and Ghan, S. J.: A parameterization of aerosol activation: 2. Multiple aerosol types, *Journal of Geophysical Research: Atmospheres*, 105, 6837–6844, <https://doi.org/10.1029/1999JD901161>, 2000.
- Ackermann, I. J., Hass, H., Memmesheimer, M., Ebel, A., Binkowski, F. S., and Shankar, U.: Modal aerosol dynamics model for Europe: development and first applications, *Atmospheric Environment*, 32, 2981–2999, [https://doi.org/https://doi.org/10.1016/S1352-2310\(98\)00006-5](https://doi.org/https://doi.org/10.1016/S1352-2310(98)00006-5), <http://www.sciencedirect.com/science/article/pii/S1352231098000065>, 1998.
- Barahona, D. and Nenes, A.: Parameterization of cirrus cloud formation in large-scale models: Homogeneous nucleation, *Journal of Geophysical Research: Atmospheres*, 113, n/a–n/a, <https://doi.org/10.1029/2007JD009355>, d11211, 2008.
- Barahona, D. and Nenes, A.: Parameterizing the competition between homogeneous and heterogeneous freezing in ice cloud formation - polydisperse ice nuclei, *Atmospheric Chemistry and Physics*, 9, 5933–5948, <https://doi.org/10.5194/acp-9-5933-2009>, <https://www.atmos-chem-phys.net/9/5933/2009/>, 2009.
- Barahona, D. and Nenes, A.: Dynamical states of low temperature cirrus, *Atmospheric Chemistry and Physics*, 11, 3757–3771, <https://doi.org/10.5194/acp-11-3757-2011>, <https://www.atmos-chem-phys.net/11/3757/2011/>, 2011.
- Barahona, D., Rodriguez, J., and Nenes, A.: Sensitivity of the global distribution of cirrus ice crystal concentration to heterogeneous freezing, *Journal of Geophysical Research: Atmospheres*, 115, n/a–n/a, <https://doi.org/10.1029/2010JD014273>, d23213, 2010.
- Barahona, D., Molod, A., Bacmeister, J., Nenes, A., Gettelman, A., Morrison, H., Phillips, V., and Eichmann, A.: Development of two-moment cloud microphysics for liquid and ice within the NASA Goddard Earth Observing System Model (GEOS-5), *Geoscientific Model Development*, 7, 1733–1766, <https://doi.org/10.5194/gmd-7-1733-2014>, <https://www.geosci-model-dev.net/7/1733/2014/>, 2014.
- Barahona, D., Molod, A., and Kalesse, H.: Direct estimation of the global distribution of vertical velocity within cirrus clouds, *Scientific Reports*, 7, 1–11, <https://doi.org/10.1038/s41598-017-07038-6>, 2017.
- Brinkop, S. and Roeckner, E.: Sensitivity of a general circulation model to parameterizations of cloud? turbulence interactions in the atmospheric boundary layer, *Tellus A*, 47, 197–220, <https://doi.org/10.1034/j.1600-0870.1995.t01-1-00004.x>, 1995.
- Cantrell, W. and Heymsfield, A.: Production of Ice in Tropospheric Clouds: A Review, *Bulletin of the American Meteorological Society*, 86, 795–807, <https://doi.org/10.1175/BAMS-86-6-795>, 2005.
- Clarke, L., Edmonds, J., Jacoby, H., Pitcher, H., Reilly, J., and Richels, R.: Scenarios of Greenhouse Gas Emissions and Atmospheric Concentrations, Sub-report 2.1A of Synthesis and Assessment Product 2.1 by the US Climate Change Science Program and the Subcommittee on Global Change Research, Department of Energy, Office of Biological & Environmental Research, Washington, DC, USA, p. 260, 2007.
- Cziczo, D. J., Stetzer, O., Worringer, A., Ebert, M., Weinbruch, S., Kamphus, M., Gallavardin, S. J., Curtius, J., Borrmann, S., Froyd, K. D., Mertes, S., Möhler, O., and Lohmann, U.: Inadvertent climate modification due to anthropogenic lead, *Nature Geoscience*, 2, 333–336, <https://doi.org/10.1038/ngeo499>, 2009.
- Cziczo, D. J., Froyd, K. D., Hoose, C., Jensen, E. J., Diao, M., Zondlo, M. A., Smith, J. B., Twohy, C. H., and Murphy, D. M.: Clarifying the Dominant Sources and Mechanisms of Cirrus Cloud Formation, *Science*, 340, 1320–1324, <https://doi.org/10.1126/science.1234145>, <http://science.sciencemag.org/content/340/6138/1320>, 2013.
- DeMott, P. J., Hill, T. C. J., McCluskey, C. S., Prather, K. A., Collins, D. B., Sullivan, R. C., Ruppel, M. J., Mason, R. H., Irish, V. E., Lee, T., Hwang, C. Y., Rhee, T. S., Snider, J. R., McMeeking, G. R., Dhaniyala, S., Lewis, E. R., Wentzell, J. J. B., Abbatt, J., Lee, C., Sultana, C. M., Ault, A. P., Axson, J. L., Diaz Martinez, M., Venero, I., Santos-Figueroa, G., Stokes, M. D., Deane, G. B., Mayol-Bracero, O. L., Grassian, V. H., Bertram, T. H., Bertram, A. K., Moffett, B. F., and Franc, G. D.: Sea spray aerosol as a unique source of



- ice nucleating particles, *Proceedings of the National Academy of Sciences*, 113, 5797–5803, <https://doi.org/10.1073/pnas.1514034112>, <http://www.pnas.org/content/113/21/5797.abstract>, 2016.
- Diehl, K. and Wurzler, S.: Heterogeneous Drop Freezing in the Immersion Mode: Model Calculations Considering Soluble and Insoluble Particles in the Drops, *Journal of the Atmospheric Sciences*, 61, 2063–2072, [https://doi.org/10.1175/1520-0469\(2004\)061<2063:HDFITI>2.0.CO;2](https://doi.org/10.1175/1520-0469(2004)061<2063:HDFITI>2.0.CO;2), 2004.
- Dietmüller, S., Jöckel, P., Tost, H., Kunze, M., Gellhorn, C., Brinkop, S., Frömming, C., Ponater, M., Steil, B., Lauer, A., and Hendricks, J.: A new radiation infrastructure for the Modular Earth Submodel System (MESSy, based on version 2.51), *Geoscientific Model Development*, 9, 2209–2222, <https://doi.org/10.5194/gmd-9-2209-2016>, <https://www.geosci-model-dev.net/9/2209/2016/>, 2016.
- Donner, L. J., O'Brien, T. A., Rieger, D., Vogel, B., and Cooke, W. F.: Are atmospheric updrafts a key to unlocking climate forcing and sensitivity?, *Atmospheric Chemistry and Physics*, 16, 12 983–12 992, <https://doi.org/10.5194/acp-16-12983-2016>, <https://www.atmos-chem-phys.net/16/12983/2016/>, 2016.
- Gottelman, A., Liu, X., Ghan, S. J., Morrison, H., Park, S., Conley, A. J., Klein, S. A., Boyle, J., Mitchell, D. L., and Li, J.-L. F.: Global simulations of ice nucleation and ice supersaturation with an improved cloud scheme in the Community Atmosphere Model, *Journal of Geophysical Research: Atmospheres*, 115, n/a–n/a, <https://doi.org/10.1029/2009JD013797>, d18216, 2010.
- Gottelman, A., Liu, X., Barahona, D., Lohmann, U., and Chen, C.: Climate impacts of ice nucleation, *Journal of Geophysical Research: Atmospheres*, 117, n/a–n/a, <https://doi.org/10.1029/2012JD017950>, d20201, 2012.
- Gultepe, I. and Heymsfield, A. J.: Introduction Ice Fog, Ice Clouds, and Remote Sensing, *Pure and Applied Geophysics*, 173, 2977–2982, <https://doi.org/10.1007/s00024-016-1380-2>, 2016.
- Guo, H., Liu, Y., Daum, P. H., Senum, G. I., and Tao, W.-K.: Characteristics of vertical velocity in marine stratocumulus: comparison of large eddy simulations with observations, *Environmental Research Letters*, 3, 1–8, <https://doi.org/10.1088/1748-9326/3/4/045020>, 2008.
- Haag, W., Kärcher, B., Ström, J., Minikin, A., Lohmann, U., Ovarlez, J., and Stohl, A.: Freezing thresholds and cirrus cloud formation mechanisms inferred from in situ measurements of relative humidity, *Atmospheric Chemistry and Physics*, 3, 1791–1806, <https://doi.org/10.5194/acp-3-1791-2003>, <https://www.atmos-chem-phys.net/3/1791/2003/>, 2003.
- Hendricks, J., Kärcher, B., and Lohmann, U.: Effects of ice nuclei on cirrus clouds in a global climate model, *Journal of Geophysical Research: Atmospheres*, 116, n/a–n/a, <https://doi.org/10.1029/2010JD015302>, d18206, 2011.
- Heymsfield, A. J., Krämer, M., Luebke, A., Brown, P., Cziczo, D. J., Franklin, C., Lawson, P., Lohmann, U., McFarquhar, G., Ulanowski, Z., and Van Tricht, K.: Cirrus Clouds, *Meteorological Monographs*, 58, 2.1–2.26, <https://doi.org/10.1175/AMSMONOGRAPHS-D-16-0010.1>, 2017.
- Hoose, C., Lohmann, U., Bennartz, R., Croft, B., and Lesins, G.: Global simulations of aerosol processing in clouds, *Atmospheric Chemistry and Physics*, 8, 6939–6963, <https://doi.org/10.5194/acp-8-6939-2008>, <https://www.atmos-chem-phys.net/8/6939/2008/>, 2008.
- IPCC: *Climate Change 2013: The Physical Science Basis*, Cambridge University Press, 1535 pp., 2013.
- Jensen, E. J., Diskin, G., Lawson, R. P., Lance, S., Bui, T. P., Hlavka, D., McGill, M., Pfister, L., Toon, O. B., and Gao, R.: Ice nucleation and dehydration in the Tropical Tropopause Layer, *Proceedings of the National Academy of Sciences*, 110, 2041–2046, <https://doi.org/10.1073/pnas.1217104110>, <http://www.pnas.org/content/110/6/2041>, 2013.
- Jöckel, P., Kerkweg, A., Pozzer, A., Sander, R., Tost, H., Riede, H., Baumgaertner, A., Gromov, S., and Kern, B.: Development cycle 2 of the Modular Earth Submodel System (MESSy2), *Geoscientific Model Development*, 3, 717–752, <https://doi.org/10.5194/gmd-3-717-2010>, <https://www.geosci-model-dev.net/3/717/2010/>, 2010.



- Kanji, Z. A., Ladino, L. A., Wex, H., Boose, Y., Burkert-Kohn, M., Cziczo, D. J., and Krämer, M.: Overview of Ice Nucleating Particles, *Meteorological Monographs*, 58, 1.1–1.33, <https://doi.org/10.1175/AMSMONOGRAPHS-D-16-0006.1>, 2017.
- Kärcher, B. and Lohmann, U.: A parameterization of cirrus cloud formation: Homogeneous freezing of supercooled aerosols, *Journal of Geophysical Research: Atmospheres*, 107, AAC 4–1–AAC 4–10, <https://doi.org/10.1029/2001JD000470>, 2002.
- 5 Kärcher, B. and Lohmann, U.: A parameterization of cirrus cloud formation: Heterogeneous freezing, *Journal of Geophysical Research: Atmospheres*, 108, n/a–n/a, <https://doi.org/10.1029/2002JD003220>, 4402, 2003.
- Kärcher, B., Hendricks, J., and Lohmann, U.: Physically based parameterization of cirrus cloud formation for use in global atmospheric models, *Journal of Geophysical Research: Atmospheres*, 111, n/a–n/a, <https://doi.org/10.1029/2005JD006219>, d01205, 2006.
- Karydis, V. A., Tsimpidi, A. P., Pozzer, A., Astitha, M., and Lelieveld, J.: Effects of mineral dust on global atmospheric nitrate concentrations, *Atmospheric Chemistry and Physics*, 16, 1491–1509, <https://doi.org/10.5194/acp-16-1491-2016>, <https://www.atmos-chem-phys.net/16/1491/2016/>, 2016.
- 10 Karydis, V. A., Tsimpidi, A. P., Bacer, S., Pozzer, A., Nenes, A., and Lelieveld, J.: Global impact of mineral dust on cloud droplet number concentration, *Atmospheric Chemistry and Physics*, 17, 5601–5621, <https://doi.org/10.5194/acp-17-5601-2017>, <https://www.atmos-chem-phys.net/17/5601/2017/>, 2017.
- 15 Kerkweg, A., Buchholz, J., Ganzeveld, L., Pozzer, A., Tost, H., and Jöckel, P.: Technical Note: An implementation of the dry removal processes DRY DEPosition and SEDimentation in the Modular Earth Submodel System (MESSy), *Atmospheric Chemistry and Physics*, 6, 4617–4632, <https://doi.org/10.5194/acp-6-4617-2006>, <https://www.atmos-chem-phys.net/6/4617/2006/>, 2006.
- Klingmüller, K., Metzger, S., Abdelkader, M., Karydis, V. A., Stenchikov, G. L., Pozzer, A., and Lelieveld, J.: Revised mineral dust emissions in the atmospheric chemistry-climate model EMAC (based on MESSy 2.52), *Geoscientific Model Development Discussions*, 2017, 1–31, <https://doi.org/10.5194/gmd-2017-160>, <https://www.geosci-model-dev-discuss.net/gmd-2017-160/>, 2017.
- 20 Koop, T., Luo, B., Tsias, A., and Peter, T.: Water activity as the determinant for homogeneous ice nucleation in aqueous solutions, *Nature*, 406, 611–614, <https://doi.org/10.1038/35020537>, 2000.
- Korolev, A., McFarquhar, G., Field, P. R., Franklin, C., Lawson, P., Wang, Z., Williams, E., Abel, S. J., Axisa, D., Borrmann, S., Crosier, J., Fugal, J., Krämer, M., Lohmann, U., Schlenzcek, O., Schnaiter, M., and Wendisch, M.: Mixed-Phase Clouds: Progress and Challenges, *Meteorological Monographs*, 58, 5.1–5.50, <https://doi.org/10.1175/AMSMONOGRAPHS-D-17-0001.1>, 2017.
- 25 Krämer, M., Rolf, C., Luebke, A., Afchine, A., Spelten, N., Costa, A., Meyer, J., Zöger, M., Smith, J., Herman, R. L., Buchholz, B., Ebert, V., Baumgardner, D., Borrmann, S., Klingebiel, M., and Avallone, L.: A microphysics guide to cirrus clouds – Part 1: Cirrus types, *Atmospheric Chemistry and Physics*, 16, 3463–3483, <https://doi.org/10.5194/acp-16-3463-2016>, <https://www.atmos-chem-phys.net/16/3463/2016/>, 2016.
- 30 Kuebbeler, M., Lohmann, U., Hendricks, J., and Kärcher, B.: Dust ice nuclei effects on cirrus clouds, *Atmospheric Chemistry and Physics*, 14, 3027–3046, <https://doi.org/10.5194/acp-14-3027-2014>, <https://www.atmos-chem-phys.net/14/3027/2014/>, 2014.
- Kumar, P., Sokolik, I. N., and Nenes, A.: Cloud condensation nuclei activity and droplet activation kinetics of wet processed regional dust samples and minerals, *Atmospheric Chemistry and Physics*, 11, 8661–8676, <https://doi.org/10.5194/acp-11-8661-2011>, <https://www.atmos-chem-phys.net/11/8661/2011/>, 2011.
- 35 Lauer, A., Eyring, V., Hendricks, J., Jöckel, P., and Lohmann, U.: Global model simulations of the impact of ocean-going ships on aerosols, clouds, and the radiation budget, *Atmospheric Chemistry and Physics*, 7, 5061–5079, <https://doi.org/10.5194/acp-7-5061-2007>, <https://www.atmos-chem-phys.net/7/5061/2007/>, 2007.



- Levkov, L., Rockel, B., Kapitza, H., and E., R.: 3D mesoscale numerical studies of cirrus and stratus clouds by their time and space evolution, *Beitr. Phys. Atmos.*, 65, 35–58, 1992.
- Lin, H. and Leaitch, W. R.: Development of an in-cloud aerosol activation parameterization for climate modelling in: Proceedings of the WMO Workshop on measurement of Cloud Properties for Forecasts of Weather, Air Quality and Climate, World Meteorological Organization, Geneva, pp. 328–335, 1997.
- 5 Liu, X. and Penner, J. E.: Ice nucleation parameterization for global models, *Meteorological Magazine*, 14, 499–514, <https://doi.org/10.1127/0941-2948/2005/0059>, 2005.
- Liu, X., Penner, J. E., Ghan, S. J., and Wang, M.: Inclusion of Ice Microphysics in the NCAR Community Atmospheric Model Version 3 (CAM3), *Journal of Climate*, 20, 4526–4547, <https://doi.org/10.1175/JCLI4264.1>, 2007.
- 10 Liu, X., Shi, X., Zhang, K., Jensen, E. J., Gettelman, A., Barahona, D., Nenes, A., and Lawson, P.: Sensitivity studies of dust ice nuclei effect on cirrus clouds with the Community Atmosphere Model CAM5, *Atmospheric Chemistry and Physics*, 12, 12 061–12 079, <https://doi.org/10.5194/acp-12-12061-2012>, <https://www.atmos-chem-phys.net/12/12061/2012/>, 2012.
- Lohmann, U. and Diehl, K.: Sensitivity Studies of the Importance of Dust Ice Nuclei for the Indirect Aerosol Effect on Stratiform Mixed-Phase Clouds, *Journal of the Atmospheric Sciences*, 63, 968–982, <https://doi.org/10.1175/JAS3662.1>, 2006.
- 15 Lohmann, U. and Hoose, C.: Sensitivity studies of different aerosol indirect effects in mixed-phase clouds, *Atmospheric Chemistry and Physics*, 9, 8917–8934, <https://doi.org/10.5194/acp-9-8917-2009>, <https://www.atmos-chem-phys.net/9/8917/2009/>, 2009.
- Lohmann, U. and Kärcher, B.: First interactive simulations of cirrus clouds formed by homogeneous freezing in the ECHAM general circulation model, *Journal of Geophysical Research: Atmospheres*, 107, AAC 8–1–AAC 8–13, <https://doi.org/10.1029/2001JD000767>, 2002.
- Lohmann, U., Feichter, J., Chuang, C. C., and Penner, J. E.: Prediction of the number of cloud droplets in the ECHAM GCM, *Journal of Geophysical Research: Atmospheres*, 104, 9169–9198, <https://doi.org/10.1029/1999JD900046>, 1999.
- 20 Lohmann, U., Stier, P., Hoose, C., Ferrachat, S., Kloster, S., Roeckner, E., and Zhang, J.: Cloud microphysics and aerosol indirect effects in the global climate model ECHAM5-HAM, *Atmospheric Chemistry and Physics*, 7, 3425–3446, <https://doi.org/10.5194/acp-7-3425-2007>, <https://www.atmos-chem-phys.net/7/3425/2007/>, 2007.
- Lohmann, U., Spichtinger, P., Jess, S., Peter, T., and Smit, H.: Cirrus cloud formation and ice supersaturated regions in a global climate model, *Environmental Research Letters*, 3, 045 022, <https://doi.org/10.1088/1748-9326/3/4/045022>, <http://stacks.iop.org/1748-9326/3/i=4/a=045022>, 2008.
- 25 Mauritsen, T., Stevens, B., Roeckner, E., Crueger, T., Esch, M., Giorgetta, M., Haak, H., Jungclaus, J., Klocke, D., Matei, D., Mikolajewicz, U., Notz, D., Pincus, R., Schmidt, H., and Tomassini, L.: Tuning the climate of a global model, *Journal of Advances in Modeling Earth Systems*, 4, n/a–n/a, <https://doi.org/10.1029/2012MS000154>, m00A01, 2012.
- 30 Meyers, M. P., DeMott, P. J., and Cotton, W. R.: New Primary Ice-Nucleation Parameterizations in an Explicit Cloud Model, *Journal of Applied Meteorology*, 31, 708–721, [https://doi.org/10.1175/1520-0450\(1992\)031<0708:NPINPI>2.0.CO;2](https://doi.org/10.1175/1520-0450(1992)031<0708:NPINPI>2.0.CO;2), 1992.
- Mülmenstädt, J., Sourdeval, O., Delanoë, J., and Quaas, J.: Frequency of occurrence of rain from liquid-, mixed-, and ice-phase clouds derived from A-Train satellite retrievals, *Geophysical Research Letters*, 42, 6502–6509, <https://doi.org/10.1002/2015GL064604>, 2015GL064604, 2015.
- 35 Phillips, V. T. J., Donner, L. J., and Garner, S. T.: Nucleation Processes in Deep Convection Simulated by a Cloud-System-Resolving Model with Double-Moment Bulk Microphysics, *Journal of the Atmospheric Sciences*, 64, 738–761, <https://doi.org/10.1175/JAS3869.1>, 2007.
- Phillips, V. T. J., DeMott, P. J., and Andronache, C.: An Empirical Parameterization of Heterogeneous Ice Nucleation for Multiple Chemical Species of Aerosol, *Journal of the Atmospheric Sciences*, 65, 2757–2783, <https://doi.org/10.1175/2007JAS2546.1>, 2008.



- Phillips, V. T. J., Demott, P. J., Andronache, C., Pratt, K. A., Prather, K. A., Subramanian, R., and Twohy, C.: Improvements to an Empirical Parameterization of Heterogeneous Ice Nucleation and Its Comparison with Observations, *Journal of the Atmospheric Sciences*, 70, 378–409, <https://doi.org/10.1175/JAS-D-12-080.1>, 2013.
- Pozzer, A., de Meij, A., Pringle, K. J., Tost, H., Doering, U. M., van Aardenne, J., and Lelieveld, J.: Distributions and regional budgets of aerosols and their precursors simulated with the EMAC chemistry-climate model, *Atmospheric Chemistry and Physics*, 12, 961–987, <https://doi.org/10.5194/acp-12-961-2012>, <https://www.atmos-chem-phys.net/12/961/2012/>, 2012.
- Pozzer, A., de Meij, A., Yoon, J., Tost, H., Georgoulias, A. K., and Astitha, M.: AOD trends during 2001–2010 from observations and model simulations, *Atmospheric Chemistry and Physics*, 15, 5521–5535, <https://doi.org/10.5194/acp-15-5521-2015>, <https://www.atmos-chem-phys.net/15/5521/2015/>, 2015.
- Pringle, K. J., Tost, H., Message, S., Steil, B., Giannadaki, D., Nenes, A., Fountoukis, C., Stier, P., Vignati, E., and Lelieveld, J.: Description and evaluation of GMXe: a new aerosol submodel for global simulations (v1), *Geoscientific Model Development*, 3, 391–412, <https://doi.org/10.5194/gmd-3-391-2010>, <https://www.geosci-model-dev.net/3/391/2010/>, 2010.
- Pruppacher, H. R. and Klett, J. D.: *Microphysics of Clouds and Precipitation*, Springer, New York, 954 pp, 1997.
- Righi, M., Hendricks, J., and Sausen, R.: The global impact of the transport sectors on atmospheric aerosol: simulations for year 2000 emissions, *Atmospheric Chemistry and Physics*, 13, 9939–9970, <https://doi.org/10.5194/acp-13-9939-2013>, <https://www.atmos-chem-phys.net/13/9939/2013/>, 2013.
- Righi, M., Hendricks, J., and Sausen, R.: The global impact of the transport sectors on atmospheric aerosol in 2030 – Part 1: Land transport and shipping, *Atmospheric Chemistry and Physics*, 15, 633–651, <https://doi.org/10.5194/acp-15-633-2015>, <https://www.atmos-chem-phys.net/15/633/2015/>, 2015.
- Righi, M., Hendricks, J., and Sausen, R.: The global impact of the transport sectors on atmospheric aerosol in 2030 – Part 2: Aviation, *Atmospheric Chemistry and Physics*, 16, 4481–4495, <https://doi.org/10.5194/acp-16-4481-2016>, <https://www.atmos-chem-phys.net/16/4481/2016/>, 2016.
- Roeckner, E., Brokopf, R., Esch, M., Giorgetta, M., Hagemann, S., Kornbluh, L., Manzini, E., Schlese, U., and Schulzweida, U.: Sensitivity of Simulated Climate to Horizontal and Vertical Resolution in the ECHAM5 Atmosphere Model, *Journal of Climate*, 19, 3771–3791, <https://doi.org/10.1175/JCLI3824.1>, 2006.
- Salzmann, M., Ming, Y., Golaz, J.-C., Ginoux, P. A., Morrison, H., Gettelman, A., Krämer, M., and Donner, L. J.: Two-moment bulk stratiform cloud microphysics in the GFDL AM3 GCM: description, evaluation, and sensitivity tests, *Atmospheric Chemistry and Physics*, 10, 8037–8064, <https://doi.org/10.5194/acp-10-8037-2010>, <https://www.atmos-chem-phys.net/10/8037/2010/>, 2010.
- Sander, R., Baumgaertner, A., Gromov, S., Harder, H., Jöckel, P., Kerkweg, A., Kubistin, D., Regelin, E., Riede, H., Sandu, A., Taraborrelli, D., Tost, H., and Xie, Z.-Q.: The atmospheric chemistry box model CAABA/MECCA-3.0, *Geoscientific Model Development*, 4, 373–380, <https://doi.org/10.5194/gmd-4-373-2011>, <https://www.geosci-model-dev.net/4/373/2011/>, 2011.
- Seinfeld, J. H., Bretherton, C., Carslaw, K. S., Coe, H., DeMott, P. J., Dunlea, E. J., Feingold, G., Ghan, S., Guenther, A. B., Kahn, R., Kraucunas, I., Kreidenweis, S. M., Molina, M. J., Nenes, A., Penner, J. E., Prather, K. A., Ramanathan, V., Ramaswamy, V., Rasch, P. J., Ravishankara, A. R., Rosenfeld, D., Stephens, G., and Wood, R.: Improving our fundamental understanding of the role of aerosol-cloud interactions in the climate system, *Proceedings of the National Academy of Sciences*, 113, 5781–5790, <https://doi.org/10.1073/pnas.1514043113>, <http://www.pnas.org/content/113/21/5781>, 2016.



- Shi, X., Liu, X., and Zhang, K.: Effects of pre-existing ice crystals on cirrus clouds and comparison between different ice nucleation parameterizations with the Community Atmosphere Model (CAM5), *Atmospheric Chemistry and Physics*, 15, 1503–1520, <https://doi.org/10.5194/acp-15-1503-2015>, <https://www.atmos-chem-phys.net/15/1503/2015/>, 2015.
- Spichtinger, P. and Cziczo, D. J.: Impact of heterogeneous ice nuclei on homogeneous freezing events in cirrus clouds, *Journal of Geophysical Research: Atmospheres*, 115, n/a–n/a, <https://doi.org/10.1029/2009JD012168>, d14208, 2010.
- 5 Stier, P., Feichter, J., Kinne, S., Kloster, S., Vignati, E., Wilson, J., Ganzeveld, L., Tegen, I., Werner, M., Balkanski, Y., Schulz, M., Boucher, O., Minikin, A., and Petzold, A.: The aerosol-climate model ECHAM5-HAM, *Atmospheric Chemistry and Physics*, 5, 1125–1156, <https://doi.org/10.5194/acp-5-1125-2005>, <https://www.atmos-chem-phys.net/5/1125/2005/>, 2005.
- Sullivan, S. C., Morales Betancourt, R., Barahona, D., and Nenes, A.: Understanding cirrus ice crystal number variability for different heterogeneous ice nucleation spectra, *Atmospheric Chemistry and Physics*, 16, 2611–2629, <https://doi.org/10.5194/acp-16-2611-2016>, <https://www.atmos-chem-phys.net/16/2611/2016/>, 2016.
- 10 Sundqvist, H., Berge, E., and Kristjansson, J. E.: Condensation and Cloud Parameterization Studies with a Mesoscale Numerical Weather Prediction Model, *Monthly Weather Review*, 117, 1641–1657, 1989.
- Tost, H.: Chemistry–climate interactions of aerosol nitrate from lightning, *Atmospheric Chemistry and Physics*, 17, 1125–1142, <https://doi.org/10.5194/acp-17-1125-2017>, <https://www.atmos-chem-phys.net/17/1125/2017/>, 2017.
- 15 Tost, H., Jöckel, P., Kerkweg, A., Sander, R., and Lelieveld, J.: Technical note: A new comprehensive SCAVenging submodel for global atmospheric chemistry modelling, *Atmospheric Chemistry and Physics*, 6, 565–574, <https://doi.org/10.5194/acp-6-565-2006>, <https://www.atmos-chem-phys.net/6/565/2006/>, 2006.
- Tsimpidi, A. P., Karydis, V. A., Pandis, S. N., and Lelieveld, J.: Global combustion sources of organic aerosols: model comparison with 84 AMS factor-analysis data sets, *Atmospheric Chemistry and Physics*, 16, 8939–8962, <https://doi.org/10.5194/acp-16-8939-2016>, <https://www.atmos-chem-phys.net/16/8939/2016/>, 2016.
- 20 van der Werf, G. R., Randerson, J. T., Giglio, L., Collatz, G. J., Mu, M., Kasibhatla, P. S., Morton, D. C., DeFries, R. S., Jin, Y., and van Leeuwen, T. T.: Global fire emissions and the contribution of deforestation, savanna, forest, agricultural, and peat fires (1997?2009), *Atmospheric Chemistry and Physics*, 10, 11 707–11 735, <https://doi.org/10.5194/acp-10-11707-2010>, <https://www.atmos-chem-phys.net/10/11707/2010/>, 2010.
- 25 Wang, M. and Penner, J. E.: Cirrus clouds in a global climate model with a statistical cirrus cloud scheme, *Atmospheric Chemistry and Physics*, 10, 5449–5474, <https://doi.org/10.5194/acp-10-5449-2010>, <https://www.atmos-chem-phys.net/10/5449/2010/>, 2010.
- Zhou, C., Penner, J. E., Lin, G., Liu, X., and Wang, M.: What controls the low ice number concentration in the upper troposphere?, *Atmospheric Chemistry and Physics*, 16, 12 411–12 424, <https://doi.org/10.5194/acp-16-12411-2016>, <https://www.atmos-chem-phys.net/16/12411/2016/>, 2016.
- 30